Carrier to envelope and dispersion control in a cavity with prism pairs

Ladan Arissian and Jean-Claude Diels
Department of Physics and Center for High Technology Materials, University of New Mexico, 1313 Goddard SE, Albuquerque, New Mexico 87106, USA
(Received 16 August 2006; published 25 January 2007)

Continuously mode-locked lasers combine a broad bandwidth with a fine comb structure that enables high resolution spectroscopy. Independent control of the pulse duration, center of gravity of the spectrum, the mode position, and spacing are essential for spectral applications and metrology. Exact analytical expressions are derived for the first, second, and third order dispersion in a cavity with a pair of intracavity prisms. The influence of cavity controls such as tilt and translation of the end mirror on the frequency comb parameters are analyzed and calculated.

DOI: 10.1103/PhysRevA.75.013814 PACS number(s): 42.60.Fc, 42.62.Eh

I. INTRODUCTION

Continuously mode-locked lasers have been since the early 70's the traditional source of a continuous train of short pulses [1]. The fact that the output consists in a train of identical pulses with fixed period lead to the realization that this source of ultrashort pulses can also become a tool of high resolution spectroscopy. Coherent interaction experiments involving pulse trains, such as the two-photon spectroscopy pioneered by Eckstein *et al.* [2], require simultaneous control of the pulse repetition rate, the mode frequency, the pulse duration, and the center of gravity of the pulse spectrum. The realization that the spectrum of a mode-locked laser can consist of rigorously equally spaced modes [3,4] led to the expression "frequency comb." The latter can be used as a "ruler" to compare and measure different frequencies across the electromagnetic spectrum. Control and stabilization of frequency combs have thus become increasingly important in physics and metrology. Intracavity prisms constitute the most versatile passive control element for mode-locked lasers. Historically, they have played an increasingly important role for the control of laser output, starting from the control of the pulse central wavelength, to the pulse duration [5,6] by providing an adjustable dispersion, and lately the pulse repetition rate [7]. For the lasers with the shortest pulse duration, there is no requirement for spectral tunability, and dispersion control is often realized with chirped mirrors [8]. This "all mirror approach" lacks the flexibility offered by a cavity with prisms, where all the parameters cited above can be controlled continuously.

Despite the fact that pairs of prisms have been used for more than two decades, there is to date no comprehensive analytical theory of the control of group delay, phase delay, and spectral bandwidth in cavities with pairs of prisms. This paper offers such an analysis for a standard laser cavity with a pair of prisms, and provides expressions for the control of dispersion, group and phase velocity, and spectrum. The essential parameters of a mode-locked comb, and their relation to the cavity parameters, are reviewed in Sec. II. In Sec. III, the equations for phase delay and group velocity dispersion for a pair of prisms are derived. It is shown that some expressions used for the prism dispersion are incorrect. Numerical examples are given for two commonly used glasses. Section IV deals with the variations of phase delay, carrier to envelope phase, and pulse spectrum introduced by a tilt and translation of the end mirror. The relative importance of all these effects will become clear with the numerical examples given at the end of this last section.

II. PARAMETERS OF A PULSE TRAIN

The *train* of pulses emitted by a mode-locked laser results from the leakage of a single pulse traveling back and forth in a cavity of constant length. The roundtrip time of the cavity is thus a constant, implying a perfectly regular comb of pulses in the time domain. In spectrum, such a pulse train is a perfect frequency comb, with teeth equally spaced at frequencies $\nu_{\text{laser},m}$. By contrast, the modes of the (non-mode-locked) laser constitute an unequal comb of frequencies $\nu_{\text{cavity},m}$ given by:

$$\nu_{\text{cavity},m} = \frac{mc}{2\sum_i n_i(\nu_{\text{cavity},m})L_i} \equiv \frac{mc}{2n(\nu_{\text{cavity},m})L}, \qquad (1)$$

where m is a positive integer and $n_i(\nu_m)L_i$ is the optical pathlength at the frequency $\nu_{\text{cavity},m}$ of the cavity element i of length L_i. We formally write $n(\nu)L=\Sigma_i n_i(\nu_{\text{cavity},m})L_i$, where L is the geometrical cavity length and $n(\nu)$ is an effective refractive index averaged over the cavity, at the frequency ν. The mode-spacing $\nu_{\text{cavity},m}-\nu_{\text{cavity},m-1}$ can be estimated by

$$\nu_{\text{cavity},m} - \nu_{\text{cavity},m-1} \approx \frac{c}{2\text{Ln}(\nu_{\text{cavity},m})}\left[1 - \frac{\nu_{\text{cavity},m}}{n(\nu_{\text{cavity},m})}\frac{dn}{d\nu}\right]$$
$$= \frac{v_g}{2L} = \frac{1}{\tau_d}. \qquad (2)$$

The time τ_d is thus the group delay through the cavity, different from the phase delay $c/2\text{Ln}(\nu_{\text{cavity},m})$. The cavity modes $\nu_{\text{cavity},m}$ and the frequency comb modes $\nu_{\text{laser},m}$ coincide at an index $m=N$. We will call ν_N this "central mode" of the mode comb, closest to the center of gravity of the pulse spectrum.

It is desirable to have a small variation of the group delay across the spectrum. All optical elements having generally a positive group velocity in the visible and near IR, a combi-

nation of elements such as a pair of prisms is desirable in order to minimize the variation of group delay across the spectrum. The procedure will be to calculate the phase shift Ψ of the light between an initial and final wave front. The group delay τ_d between these two wave fronts is given by:

$$\frac{d\Psi}{d\Omega} = \tau_d, \tag{3}$$

where $\Omega = 2\pi\nu$ is the angular optical frequency. The variation of the group delay will be investigated for a pair of prisms. First, the variation of the group delay versus frequency, which is the group velocity dispersion, will be derived exactly. Next, it will be shown that the variation of the group delay versus angle of incidence of a beam on the pair of prisms is of the same order of magnitude as the variation of the phase delay. This result applies in particular to the control of cavity roundtrip time by the tilting of an end mirror [7,9]. It will be shown also that the tilt of an end mirror results in a shift of the pulse spectrum.

III. GROUP VELOCITY CONTROL WITH PAIRS OF PRISMS

A. Frequency dependent optical path

Cavities with a single prism to control dispersion have been introduced in 1983 [5]. The adjustable positive dispersion introduced by the material of the prism, combined with negative phase modulation due to saturation of a dye solution, resulted in intracavity pulse compression down to 60 fs [5,6]. It has been demonstrated that the group velocity dispersion introduced by a *single prism* can only be positive [10] in a cavity [21]. In a configuration with two or four identical Brewster prisms however, it has been shown by Fork *et al.* [11] that the group velocity dispersion can be negative as well as positive. Numerical curves for the group velocity dispersion of prisms, pairs have been published by Petrov *et al.* [12]. A generalized theory introduced by Duarte [13–15] yields exact expressions for the angular dispersion and the beam expansion of any pairs of prisms at any incidence. The present work is limited to a pair of prisms in compensating orientation (i.e., oriented such that the input and output beams are parallel), for any wavelength. However, the interwoven contributions of angular and material dispersion to the group velocity dispersion are analyzed in detail. Exact expressions for the dispersion under arbitrary incidence are presented below. While the derivation is tedious, the result is seen to have a very simple physical interpretation.

The pair of isosceles prisms represented in Fig. 1 are oriented with their faces parallel to each other. The relative position of these prisms is defined by the two distances s and t. The position of the beam incident on the pair of prisms is defined by its angle of incidence θ_0 on the first prism, and the distance $a=OA$ from the apex O of the first prism to the point of incidence A.

The optical path $\overline{ABEFD}$ at a frequency Ω is represented by the solid line in Fig. 1, while the path for a ray upshifted by $d\Omega$ is represented by the dashed line. The beam path in

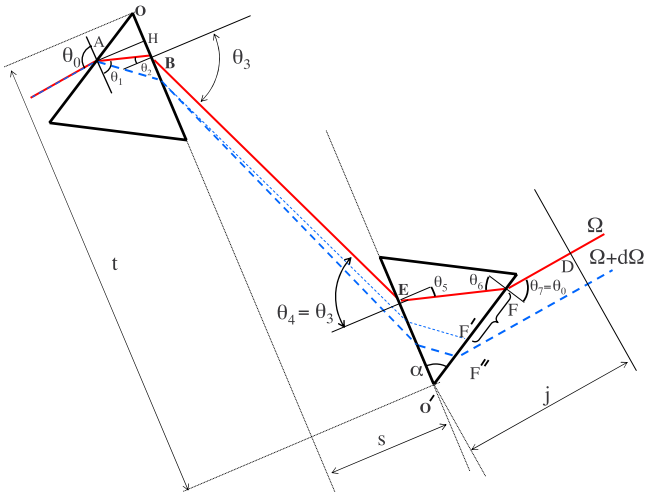

FIG. 1. (Color online) Beam propagation through a pair of parallel face identical prisms with an arbitrary apex angle α. The geometrical setup is defined by only three parameters: (1) $OA=a$ the distance of input beam to the apex of the first prism, not necessary zero, (2) t is the projection of the distance between the prisms' apexes OO' on the inner prism face, and (3) the distance s between the two inner parallel faces of the prisms, so that $L=s/\cos\theta_3$ is the beam path between the two prisms. The total propagation path is $\overline{ABEFD}$, a function of frequency. All the angles defined on the figure are related by Snell's law, where n is a function of Ω. Throughout the paper the index of refraction of the air is neglected $n_{air}=1$, the symbol n is used only for prism material.

this configuration can be divided into three sections:

$$L_g = (t - s\tan\theta_3)\frac{\sin\alpha}{\cos\theta_1},$$

$$BE = L = \frac{s}{\cos\theta_3},$$

$$\begin{aligned} w &= j - O'F\sin\theta_0 \\ &= j - [(t - s\tan\theta_3)(\cos\alpha + \sin\alpha\tan\theta_1) - a]\sin\theta_0, \end{aligned} \tag{4}$$

where L_g is total path in prisms, $BE=L$ is the propagation between the prisms, and w is the path in air to the end mirror. Note that if the two prisms were brought together (merging B and E), they constitute a slab of glass of thickness $g = L_g\cos\theta_1$. Since it is a parallel face plate of glass, the optical path L_g is independent of the distance $OA=a$.

B. Group delay

After adding all contributions to the total phase

$$\Psi = \frac{\Omega}{c}(nL_g + \overline{BE} + \overline{FD}), \tag{5}$$

we obtain, after straightforward algebra, the complete expression for the group delay through the pair of prisms (see Appendix A):

$$\frac{d\Psi}{d\Omega} = \frac{nL_g + (\overline{BE} + \overline{FD})}{c} + \frac{L_g\Omega}{c}\frac{dn}{d\Omega}. \tag{6}$$

The first term in this equation represents the travel delay at the phase velocity, and the second part of Eq. (6) is the carrier to envelope delay or $\tau_{CE}(\Omega)$ caused by the pair of prisms. The prisms are considered to be in vacuum, and the contribution to the dispersion of air is neglected.

C. Group velocity dispersion

The rigorous approach to the group velocity dispersion is to take the derivative of Eq. (6), with respect to angular frequency Ω. In this derivation, all parameters that change the optical path have to be taken into account, from the initial point A in Fig. 1 until the final point D, including the angular changes at each interface, and the displacement of the beams due to these angular changes in glass and air. The complete derivation is rather long and tedious, and is included in Appendix A. Thanks to numerous cancellations, the general result is surprisingly short and has a simple physical interpretation:

$$\frac{d^2\Psi}{d\Omega^2} = \frac{L_g}{c}\left[2\frac{dn}{d\Omega} + \Omega\frac{d^2n}{d\Omega^2}\right] - \frac{\Omega}{c}\left(\frac{s}{\cos\theta_3}\right)\left(\frac{d\theta_3}{d\Omega}\right)^2 - \frac{n\Omega L_g}{c}\left(\frac{d\theta_1}{d\Omega}\right)^2. \tag{7}$$

To understand the physical meaning of each of these terms, let us recall that the phase shift in a medium of thickness L_g and index n is $\Psi_g = \Omega n L_g/c$. The second derivative of that phase shift is the group velocity dispersion for the glass:

$$\frac{d^2\Psi_g}{d\Omega^2} = \frac{L_g}{c}\left[2\frac{dn}{d\Omega} + \Omega\frac{d^2n}{d\Omega^2}\right], \tag{8}$$

which is the first term of the complete expression (7). It has been shown [10] that a group velocity dispersion can be associated to any element that creates a wavelength dependent deflection by an angle θ:

$$\frac{d^2\Psi_\theta}{d\Omega^2} = -\frac{n\ell\Omega}{c}\left(\frac{d\theta}{d\Omega}\right)^2, \tag{9}$$

where n is the index of refraction of the medium in which the beam propagates a distance ℓ from the pivot point to the wave front of observation. In the two prism sequence of Fig. 1, A is a pivot point for the beam propagating a distance $\ell = L_g$ in the glass, and B is the pivot point for the beam propagating a distance $\ell = BE$ in air. Adding the contributions of Eq. (8) to the double contributions from Eq. (9) leads also to Eq. (7) for the group velocity dispersion of the pair of prisms. Note that expression (7) for the group velocity dispersion applies to any pair of identical isosceles prisms in the parallel face configuration represented in Fig. 1, for an arbitrary angle of incidence.

To evaluate the expression (7), it is desirable to write all derivatives in terms of the material dispersion $dn/d\Omega$. The relevant formulas are Eqs. (A5) and (A6) given in Appendix A.

Of most practical importance is the case of the minimum deviation angle ($\alpha = 2\theta_1, \theta_0 = \theta_3$) and Brewster angle prism. The simplifications to be applied in this particular case are given in Table III, Appendix A. Taking these simplifications into account the group velocity dispersion in terms of wavelength reduces to:

$$\left.\frac{d^2\Psi}{d\Omega^2}\right|_{\omega_N} = \frac{\lambda_N^3}{2\pi c^2}\left[L_g \left.\frac{d^2n}{d\lambda^2}\right|_{\lambda_N} - \left(4L + \frac{L_g}{n^3}\right)\left(\left.\frac{dn}{d\lambda}\right|_{\lambda_N}\right)^2\right], \tag{10}$$

where λ_N is the wavelength of the central mode $\nu_{laser,N}$ for which the Brewster condition is satisfied. Here $L = s/\cos\theta_3$ is the distance between the two prisms measured at the central wavelength. In many practical devices, $L \gg L_g$ and the second term of Eq. (10) reduces to $L(dn/d\lambda)^2$.

The general equation for the third order group velocity dispersion is

$$\begin{aligned}\frac{d^3\Psi}{d\Omega^3} = {} & \frac{1}{\Omega}\left(\frac{d^2\Psi}{d\Omega^2} - \frac{2L_g}{c}\frac{dn}{d\Omega}\right) + \frac{2}{c}\frac{dn}{d\Omega}\frac{dL_g}{d\Omega} + \frac{2L_g}{c}\frac{d^2n}{d\Omega^2} \\ & + \frac{L_g\Omega}{c}\frac{d^3n}{d\Omega^3} - \frac{\Omega}{c}\frac{s}{\cos^2\theta_3}(\sin\theta_3)\left(\frac{d\theta_3}{d\Omega}\right)^3 - \left(\frac{2\Omega s}{c\cos\theta_3}\right) \\ & \times\left(\frac{d\theta_3}{d\Omega}\frac{d^2\theta_3}{d\Omega^2}\right) - \left(\frac{\Omega}{c}\frac{dn}{d\Omega}L_g + \frac{n\Omega}{c}\frac{dL_g}{d\Omega}\right)\left(\frac{d\theta_1}{d\Omega}\right)^2 \\ & - \frac{n\Omega}{c}L_g\left(2\frac{d\theta_1}{d\Omega}\frac{d^2\theta_1}{d\Omega^2}\right).\end{aligned} \tag{11}$$

The following derivatives, in addition to the first order angular dispersions given by Eqs. (A5) and (A6), are needed to determine each term of this expression:

$$\frac{d^2\theta_1}{d\Omega^2} = \frac{\tan\theta_1}{n^2}\left[\frac{1}{\cos^2\theta_1} + 1\right]\left(\frac{dn}{d\Omega}\right)^2 - \frac{\tan\theta_1}{n}\frac{d^2n}{d\Omega^2}, \tag{12}$$

$$\begin{aligned}\frac{d^2\theta_3}{d\Omega^2} = {} & \frac{d}{d\Omega}\left(\frac{\sin\alpha}{\cos\theta_1\cos\theta_3}\frac{dn}{d\Omega}\right) \\ = {} & \frac{\sin\alpha}{\cos\theta_1\cos\theta_3}\left(\tan\theta_1\frac{d\theta_1}{d\Omega}\frac{dn}{d\Omega} + \tan\theta_3\frac{d\theta_3}{d\Omega}\frac{dn}{d\Omega} + \frac{d^2n}{d\Omega^2}\right).\end{aligned} \tag{13}$$

In the case of prisms at Brewster angle in the visible and near infrared, all the significant terms of the third order dispersion are contained in the first line of Eq. (11). The first term is set by second order dispersion chosen usually to compensate for positive dispersion of the cavity. Even though L_g is small, the derivative $dL_g/d\Omega$ is large, because of the change in optical path through the second prism, a change that is increasing with the separation between prisms. The last term of the first line of Eq. (11) is among the largest, because of the generally large third order dispersion of most glasses in the visible part of the spectrum. The reason is that the dispersion of glasses can be approximately modeled as the normal dispersion branch associated with a Lorentzian line (the "ultraviolet" resonance). It can easily be shown for a Lorentzian that the ratio

TABLE I. Main parameters for two prism sequences of different glasses. The index of refraction n at $\lambda=0.8$ μm, along with the first, second, and third order derivatives with respect to λ, are calculated from the Sellmeier equation. The values for B_1,B_2,B_3,C_1,C_2,C_3 are taken from the 2005 CVI catalog. The separation L between prisms is chosen so that the second order dispersion with total glass $L_g=1$ cm compensates for 500 fs^2 positive dispersion of half of the cavity round trip, from Eq. (7). The last column is the third order dispersion of the prisms separated by a distance L.

Material	n	$\left.\frac{dn}{d\lambda}\right\|_{\lambda_N}$ (μm^{-1})	$\left.\frac{d^2n}{d\lambda^2}\right\|_{\lambda_N}$ (μm^{-2})	$\left.\frac{d^3n}{d\lambda^3}\right\|_{\lambda_N}$ (μm^{-3})	L (cm)	$\left.\frac{d^3\Psi}{d\Omega^3}\right\|_{\lambda_N}$ (fs^3)
Fused silica	1.45332	-1.728×10^{-2}	3.9791×10^{-2}	−0.23898	79.36	−2048
Schott N-LAK21	1.63277	-2.5533×10^{-2}	6.8551×10^{-2}	−0.39416	47.38	−2813
Schott BK7	1.51077	-1.984×10^{-2}	4.9115×10^{-2}	−0.28906	66.13	−2304
Schott F2	1.60838	-3.495×10^{-2}	1.1549×10^{-1}	−0.64954	34.86	−4100
Schott SF2	1.62719	-3.7105×10^{-2}	1.2449×10^{-1}	−0.69916	32.56	−4339
Schott N-SF10	1.71129	-4.9957×10^{-2}	1.7159×10^{-1}	−0.97956	22.66	−5458
Schott N-SF11	1.76312	-5.4753×10^{-2}	1.90595×10^{-1}	−1.0993	20.45	−5930
CaF_2	1.43053	-1.046×10^{-2}	3.0709×10^{-2}	−0.16835	196.12	−2124

$$r=\frac{\dfrac{d^3n/d\Omega^3}{d^2n/d\Omega^2}}{\dfrac{d^2n/d\Omega^2}{dn/d\Omega}}=6, \tag{14}$$

demonstrating an increased influence of the third order dispersion. This model applies only to wavelengths short enough that the influence of the infrared absorption bands cannot be felt. An appropriate wavelength for this model is 620 nm for fused silica. Using the values of the indices and their derivatives from Ref. [10], Table 2.1, one finds the value of this ratio to be $r=5.7$. The second and third line of Eq. (11) can be neglected because the angular third order dispersion terms are very small.

The study of the prism dispersion in a linear cavity can be applied to the similar case of four prisms in a ring. In both cases the value for the dispersion has to be multiplied by two due to double passage through the prism pairs. In a linear cavity a prism is usually translated along the bisector of the apex angle α to adjust the dispersion through the glass for desired group velocity dispersion in the cavity.

D. Typical cases

Fused silica prisms are most often used for the generation of very short pulses, because of their low third order dispersion as compared to other materials. If a high repetition rate is desired, materials such as LAK21, BK7, SF6 or SF14 glasses are used, allowing for a more compact design. Table I shows the index of refraction and the first, second, and third derivative of n with respect to wavelength (μm). The coefficients of the Sellmeier equation are taken from the CVI catalog (2005) [22]. The laser is operating at $\lambda_N=800$ nm. It is assumed that the intracavity elements—including the gain medium—introduce a group velocity dispersion of 500 fs^2 (for a half cavity round trip), and that the total optical path in the glass is $L_g=1$ cm. The minimum separation between prisms L is calculated, for which the total cavity second order dispersion is zero. Operation of the laser requires a slightly negative dispersion to compensate for the self-phase modulation (Kerr effect) in the gain medium. The third order dispersion due to the prism pair is calculated from Eq. (11).

E. Evaluation of these results in the context of previous work

The most commonly cited equation to evaluate the dispersion of a pair of prisms is that contained in the article by Fork *et al.* [11], which, limited to the Brewster angle prisms, reads:

$$\frac{d^2P}{d\lambda^2}=4L\left\{\left[\frac{d^2n}{d\lambda^2}+\left(2n-\frac{1}{n^3}\right)\left(\frac{dn}{d\lambda}\right)^2\right]\sin\Delta\theta_3-2\left(\frac{dn}{d\lambda}\right)^2\cos\Delta\theta_3\right\}. \tag{15}$$

In this equation $P=2L\cos\Delta\theta_3$ and L is the distance between the two prisms. In this calculation $\Delta\theta_3$ is defined by the assumption that $L\sin\Delta\theta_3=2$ mm, or twice the beam size. The main difference between Eq. (7) or Eq. (10) and the results of Ref. [11] are:

(i) Equation (15) is only for the case of tip to tip propagation in the prisms; the positive material dispersion and the angular dispersion of the beam propagating a distance L_g in the prisms are neglected.

(ii) In Eq. (15) the only optical path considered is L or the path between the two prisms; the beam displacement after the second prism is not calculated. The angular and transverse displacements of the beam after the second prism contribute to a wavelength dependent change in optical path, as shown in Appendix A.

(iii) Even if it were correct, the term in $\sin\Delta\theta_3$ should cancel in the four prism configuration of a ring cavity, or double passage through the pair of prisms in a linear cavity, as the beam folds through the third and fourth prism.

(iv) The correct expression for group velocity dispersion is $d^2\Psi/d\Omega^2$, where $\Psi=(\Omega n/c)P$, and not $d^2P/d\lambda^2$.

(v) A numerical example might help to complete the evaluation of the simplifications made in Reference [11]. Equation (15) applied to a pair of fused silica prisms for 800 nm pulses leads to a minimum separation between prisms of $L=138$ mm, *even in the absence of any positive dispersion element*. The calculation from Eq. (10) for a similar case of zero passage through glass, $L_g=0$, will result in negative dispersion for any positive separation L. Note that the separation L between the prisms can only contribute in negative dispersion, as shown by Eq. (7). Equation (15) instead implies that the separation between the prisms L has both a positive and negative effect.

IV. EFFECTS OF A TILT AND TRANSLATION OF THE END MIRROR

Since the publications of Reichert [7], it seems to be an accepted concept that a tilt of the end mirror modifies exclusively the group velocity of the pulse. This confidence—expressed in numerous articles (see for instance Refs. [16,17]), stems from a commonly referenced article [9]. This particular paper does not relate to a pair of prisms, but to a combination of a single grating with a lens (the grating being placed in the focal plane of the achromatic lens), facing a pivoting mirror in the opposite focal plane. In the stabilization loop of a laser, it is desirable to have independent control of group and phase delays. As pointed out in Ref. [18], such a goal can be rigorously achieved in a synchronously pumped optical parametric oscillator (OPO), where the group delay is uniquely determined by the pump cavity length, and the phase delay solely by the OPO (signal) cavity length. The common technique to circumvent the absence of orthogonal control parameters is to apply two linear combinations of the error signals for the phase and group delays, to two different (but not orthogonal) control elements of the laser [19,20]. The two control elements chosen in the two cited references [16,17] are the tilt of an end mirror following a prism sequence, and the cavity length. The calculations that follow lead to a determination of the response of these two actuators (tilt and translation), in terms of a change in phase and group delays, and also spectral shift. It will be shown that, contrary to widespread belief, the tilt of the end mirror of a two prism sequence is not equivalent to the "mechanical scanning delay line" [9]. While there is a change in group delay, there is also an important change in phase delay and a shift of the spectrum, as the end mirror (after a prism pair) is tilted. Understanding this optical arrangement is important, considering the high precision that is required for today's metrology.

A. The cavity configuration and effects of the end mirror tilt

The cavity under consideration is a standard arrangement consisting in a flat output coupler, a gain section comprising the Brewster angle crystal between two curved mirrors of equal focal distance, followed by a pair of prisms, and finally an end cavity mirror M_1, as shown in Fig. 2(a). The combination of output coupler and the two curved mirrors can be replaced by a curved end cavity mirror M_2 of radius of R_{cavity} located at a distance L_{cavity} from the end mirror [Fig. 2(b)]. A prism sequence (not shown in the figure) is generally located between the tilting (flat) end mirror M_1 and the gain section. If the end mirror M_1 is tilted about an axis not located at the point of incidence of the beam, rotation by an angle $\Delta\theta$ leads, to first order, to a cavity elongation ΔL as sketched in Fig. 2(c). This effect is only of second order (in $\Delta\theta$) if the axis of rotation is at the point of incidence, as in Fig. 2(d).

A displacement h of the beam parallel to itself does not change the optical path through the prisms, hence will not have any effect on phase or group delay. However, after a tilt of mirror M_1, the beam moves to remain along the common normal to both M_1 and the "equivalent" mirror M_2, hence along a line through the center of curvature C of mirror M_2. As shown in Fig. 2(e), the intracavity laser beam is not only rotated by $\Delta\theta$ on mirror M_1, but also translated by $h=\Delta\theta\times(R_{\text{cavity}}-L_{\text{cavity}})$. Note that there is a corresponding cavity elongation $h\Delta\theta=(R_{\text{cavity}}-L_{\text{cavity}})\times(\Delta\theta)^2$, which is second order with respect to $\Delta\theta$. In a typical example of $R_{\text{cavity}}=2$ m and $L_{\text{cavity}}=1$ m, the additional delay is $h\Delta\theta/c=3.3(\Delta\theta)^2$ fs, for $\Delta\theta$ expressed in milliradian, and h in mm.

B. Spectral shift

It is clear that a translation of an end mirror displaces the cavity modes, without affecting the overall spectral envelope of the laser.

In a solid state laser, the alignment of the cavity mode inside the gain rod, with respect to the focal volume of the pump beam, provides the wavelength selection [Fig. 2(f)]. The gain line inside the crystal is oriented at the (fixed) internal Brewster angle $\theta_{Bcr}=\arctan(1/n)$. The external angle θ_i, however, has a variation $\Delta\theta$ due to the tilt of the end mirror M_1. Snell's law applied to the Brewster interface is:

$$\sin\theta_i = n\sin\theta_{Bcr}. \tag{16}$$

Differentiating:

$$\cos\theta_i\Delta\theta = \frac{dn}{d\lambda}\sin\theta_{Bcr}\Delta\lambda. \tag{17}$$

Therefore:

$$\Delta\lambda = \frac{1}{\dfrac{dn}{d\lambda}}\Delta\theta. \tag{18}$$

The spectral shift due to 1 mrad rotation of the end mirror, for the Ti:sapphire ($dn/d\lambda=-0.01805\ \mu\text{m}^{-1}$ at 0.8 μm), is 55 nm. This effect is thus quite large, and cannot be neglected if the laser is to be tuned to an atomic or molecular transition.

C. Change in group and phase delay due to tilt and translation

To a tilt of the end mirror M_1 by an angle $\Delta\theta$ corresponds a displacement of the beam that can be decomposed into a

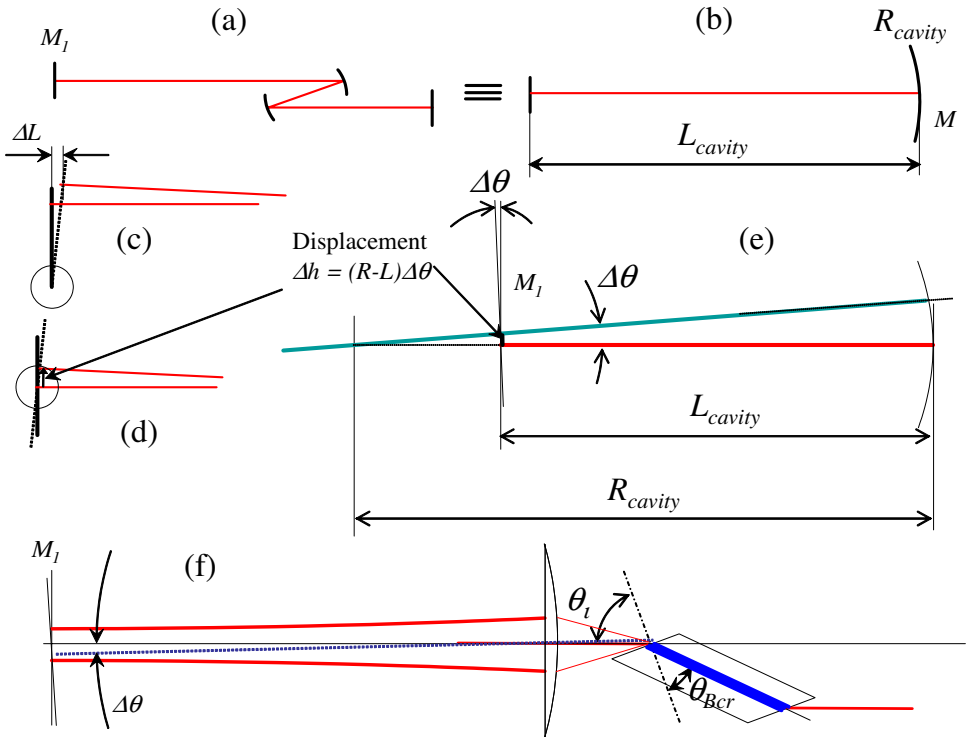

FIG. 2. (Color online) Representation of a standard cavity of a femtosecond solid state laser. In (a), overall cavity configuration, excluding the prisms, which is equivalent to the two mirror cavity shown in (b). If the axis of rotation of the tilting mirror is not positioned exactly at the point of incidence of the intracavity beam, the effect of a mirror tilt results also in a cavity length change ΔL (c). This cavity length change is zero to first order when the rotation axis passes through the point of incidence (d). In (e), the equivalent two mirror cavity is used to illustrate the displacement h of the beam on mirror M_1, due to a tilt by an angle $\Delta\theta$. In (f), only a portion of the cavity extending from the tilting mirror M_1 to the Brewster angle laser rod (represented enlarged for clarity) is sketched. The envelope of the Gaussian mode is shown. The lasing mode has a waist at M_1 and inside the gain rod. The axis of the tilted mode is represented by the dotted line.

rotation $\Delta\theta$ and a translation by h of the incidence point on the mirror. In evaluating the effect of this motion of the beam on the prism sequence, we can eliminate the effect of translation. Indeed, it can easily be seen that the optical phase of the beam passing a two prism sequence is independent of a beam translation normal to the wave front. It is therefore sufficient to study the change in optical path, for a beam tilted at the pivot point by an angle $\Delta\theta$, as shown in Fig. 3.

D. Tilting of the end mirror

The path lengths are as mentioned in Eq. (4) with the addition of an initial path in air:

$$u = i - OA \sin\theta_0 = i - a \sin\theta_0. \tag{19}$$

Note that A is no longer a pivot point. The proper pivot axis is in the plane of the rotating mirror. The total change in optical phase, per unit angle, is:

$$\frac{d\Psi}{d\theta_0} = \frac{\Omega}{c}\left[(t - s\tan\theta_3)\frac{-\cos\theta_0\cos\theta_2}{\cos\theta_1}\right]. \tag{20}$$

Note that neither "a" nor the variation in a do contribute to the change in optical phase, as these variations cancel out (Appendix B). For the particular case of minimum deviation ($\theta_3=\theta_0$ and $\theta_1=\theta_2=\alpha/2$) and Brewster incidence ($\tan\theta_0=n$), the variation of optical phase due to tilt reduces to:

$$\frac{d\Psi}{d\theta_0} = \frac{\Omega}{c}\left[(t - sn)\frac{-\dfrac{1}{\sqrt{1+n^2}}\dfrac{n}{\sqrt{1+n^2}}}{\dfrac{n}{\sqrt{1+n^2}}}\right] \tag{21}$$

or

$$\frac{d\Psi}{d\theta_0} = \frac{-\pi}{\lambda}L_g, \tag{22}$$

where L_g is the total length of propagation in the glass. For a laser at 800 nm propagating to total amount of glass of 1 cm, the phase change is $(6.25\times 2\pi)/\text{mrad}$.

Let us next proceed to a calculation of the variation in *group delay* due to the tilt. Adding the air-path contribution from the pivot point to the first prism to Eq. (6) leads to the following expression for the group delay:

$$\frac{d\Psi}{d\Omega} = \frac{OPL(u + ABEF + w)}{c} + \frac{L_g\Omega}{c}\frac{dn}{d\Omega}. \tag{23}$$

As in the case of Eq. (6), the group delay consists in two parts: the left term being the phase delay, and the right term the carrier to envelope delay. The group delay variation, by

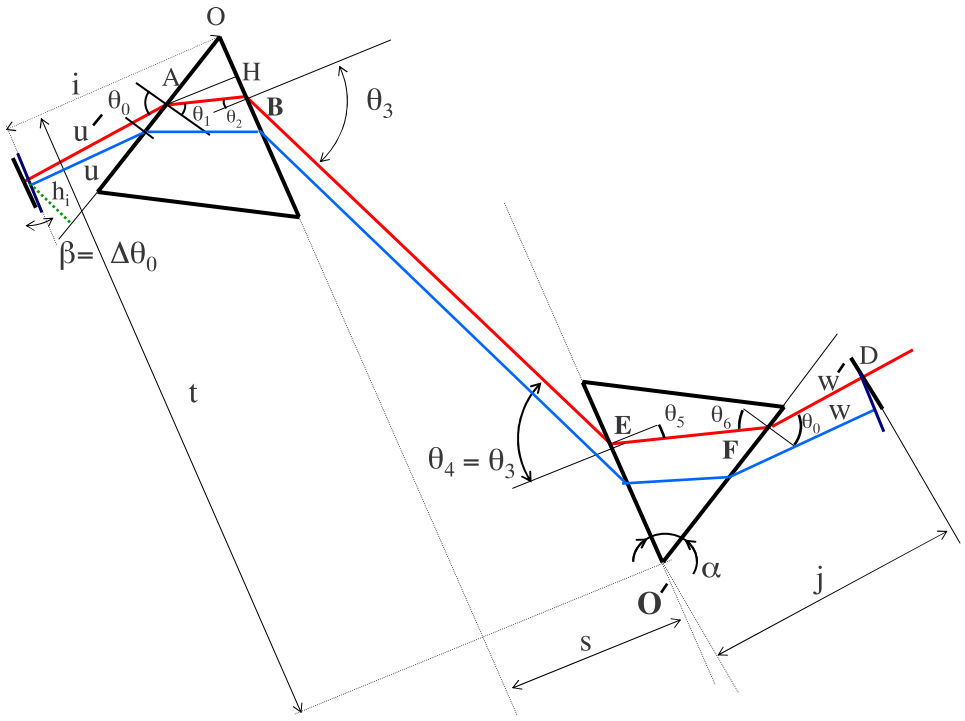

FIG. 3. (Color online) The figure shows the beam propagation through prisms and air. The dashed trajectory is the initial beam and the dotted one is the shifted beam due to a *negative* tilt of the mirror at far left. u and w are the path in air before and after passing through the prism pairs, respectively. BE is the path in air between the two parallel face prisms. $L_g = AB + EF$ is the total travel through two prisms. t is the apex to apex distance between prisms projected on an internal face, and s is the parallel internal face distances. $OA = a$ is the distance of the beam input trajectory to the apex of the prism.

tilting the end mirror in a linear cavity with prism pairs, is

$$\frac{d}{d\theta_0}\frac{d\Psi}{d\Omega} = \frac{1}{c}\left[(t - s\tan\theta_3)\frac{-\cos\theta_0\cos\theta_2}{\cos\theta_1}\right] + \frac{\Omega}{c}\frac{dn}{d\Omega}\left[\frac{s}{\cos^2\theta_3}\frac{\cos\theta_2\cos\theta_0}{\cos\theta_1\cos\theta_3}\frac{\sin\alpha}{\cos\theta_1} + (t - s\tan\theta_3)\frac{\sin\alpha\sin\theta_1}{\cos^2\theta_1}\frac{\cos\theta_0}{n\cos\theta_1}\right]. \quad (24)$$

This expression simplifies in the case of minimum deviation and Brewster prism:

$$\frac{d}{d\theta_0}\frac{d\Psi}{d\Omega} = \frac{-L_g}{2c} + \frac{\Omega}{c}\frac{dn}{d\Omega}\left[2L + \frac{L_g}{n^3}\right], \quad (25)$$

where the total variation with angle of the group delay is expressed in two terms, the left term being the angular variation of phase delay, and the second the angular variation of carrier to envelope (CEO) delay.

The material parameters were given in Table I, for the case of a laser operating at $\lambda_N = 800$ nm. Table II lists the values of phase delay, CEO delay, and group delay, due to the rotation of an end mirror, for the distance L calculated in Table I. The phase delay does not include the second order contribution $(R_{\text{cavity}} - L_{\text{cavity}}) \times (\Delta\theta)^2$ mentioned at the beginning of Sec. IV A.

E. Translation of the end mirror

For a pulse propagating in a homogeneous medium of index n, the group delay is defined by:

$$\frac{dk}{d\Omega} = \frac{1}{v_g} = \frac{1}{c}\left(n - \lambda\frac{dn}{d\lambda}\right). \quad (26)$$

If the end mirror of the cavity is translated (perpendicular to the phase front) by ΔL, the change in length occurs only in air, and the change in group delay is simply the phase delay:

$$\Delta L/c. \quad (27)$$

A change in cavity length of $\Delta L = 5$ μm corresponds to the phase change due to 1 mrad rotation $(6.25 \times 2\pi)$.

V. CONCLUSION

Complete expressions were derived for the second and third order dispersion introduced by pairs of isosceles prisms at any angle of incidence. It is shown that the short path in glass, often neglected, leads to the dominant terms in the

TABLE II. Phase, CEO delay, and group delay due to rotation of an end mirror. Prism pair configurations are as mentioned in Table I.

Material	Phase delay (fs/mrad)	CEO delay (fs/mrad)	Group delay (fs/mrad)
Fused silica	−16.7	73.4	56.7
Schott N-LAK21	−16.7	64.7	48.1
Schott BK7	−16.7	70.2	53.5
Schott F2	−16.7	65.3	48.6
Schott SF2	−16.7	64.7	48.0
Schott N-SF10	−16.7	60.7	44.0
Schott N-SF11	−16.7	60.0	43.3
CaF_2	−16.7	109.6	92.9

third order dispersion. Contrary to accepted belief, tilt of the mirrors do not provide control of group delay, independent of phase delay. In addition, the tilt results in a large spectral shift, as we have observed in several Ti:sapphire laser cavities. Fused silica prisms are the best solution for dispersion (smallest third order) and tilt (largest ratio of group to phase delay). Unfortunately, the use of fused silica requires longer cavities. For cavities with very small dispersion, it may be advantageous to use small apex angle prisms (rather than Brewster prisms), which result in a smaller third order dispersion, and a smaller phase delay upon tilt.

ACKNOWLEDGMENT

This work was supported by the National Science Foundation under Grant Number ECS 0601612.

APPENDIX A: DISPERSION FOR A PAIR OF PRISMS

This appendix is to show and share the detailed calculation of the group delay and first and second order dispersion for a pair of identical parallel prisms. The calculations are made for the general case, unless specified in Brewster or minimum deviation.

1. Group delay

From Fig. 1 the group delay is:

$$\begin{aligned}\frac{d\Psi}{d\Omega} &= \frac{d}{d\Omega}\left(\frac{\Omega n L_g}{c}\right) + \frac{d}{d\Omega}\left(\frac{\Omega\overline{BE}}{c}\right) + \frac{d}{d\Omega}\left(\frac{\Omega\overline{FD}}{c}\right)\\ &= \frac{nL_g}{c} + \frac{(\overline{BE}+\overline{FD})}{c} + \frac{L_g\Omega}{c}\frac{dn}{d\Omega} + \frac{n\Omega L_g}{c}\tan\theta_1\frac{d\theta_1}{d\Omega}\\ &\quad + \left\{-\frac{n\Omega s}{c\cos^2\theta_3}\frac{\sin\alpha}{\cos\theta_1} + \frac{\Omega s}{c\cos\theta_3}\tan\theta_3\right.\\ &\quad \left. + \frac{n\Omega s}{c\cos^2\theta_3}\left[\cos\alpha\sin\theta_1 + \frac{\sin\alpha\sin^2\theta_1}{\cos\theta_1}\right]\right\}\frac{d\theta_3}{d\Omega}\\ &\quad - \frac{n\Omega}{c}[t - s\tan\theta_3]\frac{\sin\alpha\sin\theta_1}{\cos^2\theta_1}\frac{d\theta_1}{d\Omega}\\ &= \frac{OPL(ABEFD)}{c} + \frac{L_g\Omega}{c}\frac{dn}{d\Omega} + \left(\frac{\Omega s}{c\cos^2\theta_3}\right)\\ &\quad \times(-n\sin\alpha\cos\theta_1 + \cos\theta_3\tan\theta_3\\ &\quad + n\cos\alpha\sin\theta_1)\frac{d\theta_3}{d\Omega},\end{aligned} \tag{A1}$$

where we have defined the optical path length $OPL(ABEFD) = nL_g + (\overline{BE}+\overline{FD})$. The factor preceding $d\theta_3/d\Omega$ cancels, since $\alpha = \theta_1 + \theta_2$ the term

$$\cos\alpha\sin\theta_1 - \sin\alpha\cos\theta_1 + \frac{\sin\theta_3}{n} = \sin(\theta_1 - \alpha) + \sin\theta_2 \tag{A2}$$

TABLE III. Simplifications for Brewster prisms at minimum deviation angle.

$\tan\theta_0 = n$	$\sin\theta_0 = \cos\theta_1 = \frac{n}{\sqrt{1+n^2}}$
$\tan\theta_1 = \frac{1}{n}$	$\cos\theta_0 = \sin\theta_1 = \frac{1}{\sqrt{1+n^2}}$
$\sin\alpha = \frac{2n}{n^2+1}$	

vanishes. The complete expression for the group delay through the pair of prisms reduces to:

$$\frac{d\Psi}{d\Omega} = \frac{OPL(ABEFD)}{c} + \frac{L_g\Omega}{c}\frac{dn}{d\Omega} \tag{A3}$$

2. First order group velocity dispersion

The second derivative of the phase, obtained by taking the derivative of Eq. (A3), is:

$$\begin{aligned}\frac{d^2\Psi}{d\Omega^2} &= \frac{L_g}{c}\left[2\frac{dn}{d\Omega} + \Omega\frac{d^2n}{d\Omega^2}\right] - \frac{\Omega}{c\cos\theta_1}\frac{dn}{d\Omega}\frac{s\sin\alpha}{\cos^2\theta_3}\frac{d\theta_3}{d\Omega}\\ &\quad + \frac{\Omega}{c}\frac{dn}{d\Omega}\left(L_g\tan\theta_1\frac{d\theta_1}{d\Omega}\right).\end{aligned} \tag{A4}$$

The derivatives with respect to Ω are related. By differentiating Snell's law for the first interface:

$$\frac{d\theta_1}{d\Omega} = -\frac{\tan\theta_1}{n}\frac{dn}{d\Omega} = -\frac{d\theta_2}{d\Omega}. \tag{A5}$$

For the second interface, taking the previous relation into account, we find:

$$\cos\theta_3\frac{d\theta_3}{d\Omega} = n\cos\theta_2\frac{d\theta_2}{d\Omega} + \sin\theta_2\frac{dn}{d\Omega},$$

$$\frac{d\theta_3}{d\Omega} = \frac{\sin\alpha}{\cos\theta_1\cos\theta_3}\frac{dn}{d\Omega}. \tag{A6}$$

In these equations, one can easily make the substitution $\theta_2 = \alpha - \theta_1$, and $\theta_1 = \arcsin(n^{-1}\sin\theta_0)$.

The second order dispersion Eq. (A4) reduces to an easily interpretable form:

$$\begin{aligned}\frac{d^2\Psi}{d\Omega^2} &= \frac{L_g}{c}\left[2\frac{dn}{d\Omega} + \Omega\frac{d^2n}{d\Omega^2}\right] - \frac{\Omega}{c}\left(\frac{s}{\cos\theta_3}\right)\left(\frac{d\theta_3}{d\Omega}\right)^2\\ &\quad - \frac{n\Omega}{c}L_g\left(\frac{d\theta_1}{d\Omega}\right)^2.\end{aligned} \tag{34}$$

This expression can be simplified for the case of incidence at the minimum deviation angle (symmetric beam path through

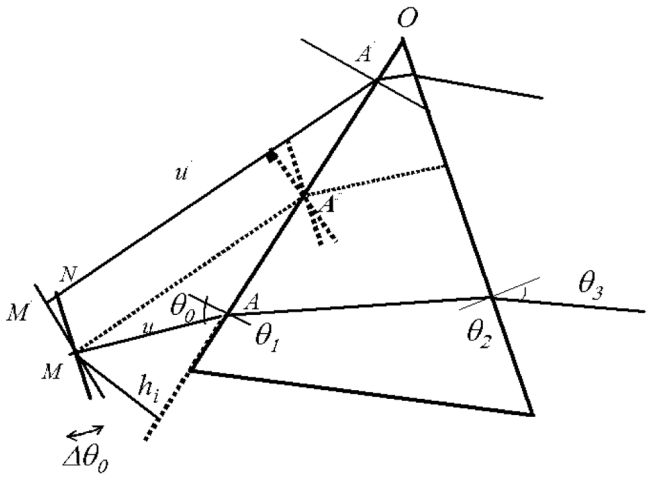

FIG. 4. The figure shows the change in angles and optical paths due to the rotation of the end mirror. The figure shows how the spot will displace on the mirror with rotation as well. The solid line trajectory MA is the beam path in initial position, and the solid line $M'A'$ is the modified beam path after the rotation. The dotted line trajectory MA'' is the intermediate step (ignoring the beam displacement on the mirror) to calculate the change in OA to OA'.

the prism for $\Omega=\omega_N$). In addition, for minimum intracavity loss, the prisms will generally be cut with an apex angle α such that the minimum deviation angle is also the Brewster angle. The particular values of the angles are given in Table III. We can also make the substitutions $d\theta_1/d\Omega=-1/n^2 dn/d\Omega$, and $d\theta_3/d\Omega=2dn/d\Omega$. With these simplifications, the total second order dispersion in this case becomes:

$$\left.\frac{d^2\Psi}{d\Omega^2}\right|_{\omega_N}=\frac{L_g}{c}\left[2\left.\frac{dn}{d\Omega}\right|_{\omega_N}+\omega_N\left.\frac{d^2n}{d\Omega^2}\right|_{\omega_N}\right]-\frac{\omega_N}{c}\left(4L+\frac{L_g}{n^3}\right)\left(\left.\frac{dn}{d\Omega}\right|_{\omega_N}\right)^2, \tag{A7}$$

where we have introduced the distance between the two prisms measured along the central wavelength $L=s/\cos\theta_3$. In terms of wavelength:

$$\left.\frac{d^2\Psi}{d\Omega^2}\right|_{\lambda_N}=\frac{\lambda_N^3}{2\pi c^2}\left[L_g\left.\frac{d^2n}{d\lambda^2}\right|_{\lambda_N}-\left(4L+\frac{L_g}{n^3}\right)\left(\left.\frac{dn}{d\lambda}\right|_{\lambda_N}\right)^2\right]. \tag{A8}$$

APPENDIX B: TILTING THE END MIRROR

The changes in paths and angles can be monitored by application of the Snell's law. Let us look at the change of the optical path when the end mirror is rotated by angle $\Delta\theta_0$ from the pivot point positioned at a distance h_i from the prism face.

(i) The change in path length to the first prism surface u: Note that due to the rotation of the mirror the laser spot will move on the surface of the mirror by $\Delta m=(R_{\text{cavity}}-L_{\text{cavity}})\Delta\theta_0$, where L_{cavity} is the cavity length and R_{cavity} is the effective curvature of the cavity mirrors. In the case of a concentric cavity at the limit of stability, the tilting mirror is located at the center of curvature and is equal to R_{cavity}, that is the only case where the laser spot will not move on the mirror with rotation. In Fig. 4, the pivot point is the initial laser beam spot at M, the laser spots move to M' and the beam path to the prism changes from u to u'. This change can be decomposed to change due to the rotation or change in the incident angle and a change due to translation of the spot on the mirror. The differential path change before the prism (neglecting second order terms) is:

$$\frac{du}{d\theta_0}=\frac{\delta u}{\delta h}\frac{\delta h}{\delta\theta_0}+\frac{\delta u}{\delta\theta_0}\approx\frac{(R_{\text{cavity}}-L_{\text{cavity}})}{\cos\theta_0}+\frac{h_i\sin\theta_0}{\cos^2\theta_0}. \tag{B1}$$

In the above expression, the first term, representing a translation of the beam, does not contribute to any optical path change through the prism combination. The second one is due to the rotation (or change in angle of incidence on the mirror). The spot shift due to the mirror tilt will contribute to the variation of parameter a.

(ii) Change in angles: The change in angles due to the mirror tilt starts from θ_0, and is transferred to all the other angles as follows:

$$d\theta_1=\frac{\cos\theta_0}{n\cos\theta_1}d\theta_0,$$

$$d\theta_2=-d\theta_1,$$

$$d\theta_3=\frac{n\cos\theta_2}{\cos\theta_3}d\theta_2=-\frac{\cos\theta_2\cos\theta_0}{\cos\theta_1\cos\theta_3}d\theta_0. \tag{B2}$$

(iii) Propagation in air between the two parallel faces of the prisms BB':

$$\frac{d(BE)}{d\theta_0}=s\frac{\sin\theta_3}{\cos^2\theta_3}\frac{-\cos\theta_2\cos\theta_0}{\cos\theta_1\cos\theta_3}. \tag{B3}$$

(iv) The total propagation in glass (prisms) L_g:

$$\frac{dL_g}{d\theta_0}=\frac{s}{\cos^2\theta_3}\frac{\cos\theta_2\cos\theta_0}{\cos\theta_1\cos\theta_3}\frac{\sin\alpha}{\cos\theta_1}+(t-s\tan\theta_3)\frac{\sin\alpha\sin\theta_1}{\cos^2\theta_1}\frac{\cos\theta_0}{n\cos\theta_1}. \tag{B4}$$

(v) The change in path in air outside the two prisms or $u+w$: Using Eqs. (4) and (B2)

$$\frac{d(u+w)}{d\theta_0}=[-\cos\theta_0(t-s\tan\theta_3)](\cos\alpha+\sin\alpha\tan\theta_1)+s\frac{\sin\theta_0}{\cos^2\theta_3}\frac{-\cos\theta_2\cos\theta_0}{\cos\theta_1\cos\theta_3}(\cos\alpha+\sin\alpha\tan\theta_1)-\sin\theta_0(t-s\tan\theta_3)\frac{\sin\alpha}{\cos^2\theta_1}\frac{\cos\theta_0}{n\cos\theta_1}. \tag{B5}$$

There is no dependence on a or the position of the beam on the first prism in the combination of $u+w$. In the parallel

prism pair configuration, if the beam moves away from the apex of the first prism, it will result in the beam spot moving closer to the apex of the second one. The same opposite variation corresponds to the path before the first and after the second prism (Fig. 4).

The total change in phase Ψ due to the mirror rotation is:

$$\frac{d\Psi}{d\theta_0} = \frac{\Omega}{c}\left\{(t - s\tan\theta_3)\left[\frac{n\sin\alpha\sin\theta_1}{\cos^2\theta_1}\frac{\cos\theta_0}{n\cos\theta_1} - \cos\theta_0(\cos\alpha + \sin\alpha\tan\theta_1) - \sin\theta_0\frac{\sin\alpha}{\cos^2\theta_1}\frac{\cos\theta_0}{n\cos\theta_1}\right] + \frac{s}{\cos^3\theta_3}\frac{\cos\theta_0\cos\theta_2}{\cos\theta_1} \times \left[-\sin\theta_0(\cos\alpha + \sin\alpha\tan\theta_1) - \sin\theta_3 + \frac{n\sin\alpha}{\cos\theta_1}\right]\right\}. \tag{B6}$$

The first two lines can be simplified, using the equalities $n\sin\theta_1 = \sin\theta_0$ and $\alpha = \theta_2 + \theta_1$. The same considerations will result in a vanishing third line of Eq. (B6). The group delay due to the mirror tilt is thus:

$$\frac{d\Psi}{d\theta_0} = \frac{\Omega}{c}\left[(t - s\tan\theta_3)\frac{-\cos\theta_0\cos\theta_2}{\cos\theta_1}\right]. \tag{B7}$$

[1] I. S. Ruddock and D. J. Bradley, Appl. Phys. Lett. **29**, 296 (1976).
[2] J. N. Eckstein, A. I. Ferguson, and T. W. Hänsch, Phys. Rev. Lett. **40**, 847 (1978).
[3] R. J. Jones, J. C. Diels, J. Jasapara, and W. Rudolph, Opt. Commun. **175**, 409 (2000).
[4] T. Udem, J. Reichert, R. Holzwarth, and T. Hänsch, Opt. Lett. **24**, 881 (1999).
[5] W. Dietel, J. J. Fontaine, and J.-C. Diels, Opt. Lett. **8**, 4 (1983).
[6] J. J. Fontaine, W. Dietel, and J.-C. Diels, IEEE J. Quantum Electron. **QE-19**, 1467 (1983).
[7] J. Reichert, R. Holzwarth, T. Udem, and T. W. Hänsch, Opt. Commun. **172**, 59 (1999).
[8] F. X. Kärtner, N. Matuschek, T. Schibli, U. Keller, H. A. Haus, C. Heine, R. Morf, V. Scheuer, M. Tilsch, and T. Tschudi, Opt. Lett. **22**, 831 (1997).
[9] K. F. Kwong, D. Yankelevich, K. C. Chu, J. P. Heritage, and A. Dienes, Opt. Lett. **18**, 558 (1993).
[10] J.-C. Diels and W. Rudolph, *Ultrashort Laser Pulse Phenomena* (Elsevier, Boston, 2006).
[11] R. L. Fork, O. E. Martinez, and J. P. Gordon, Opt. Lett. **9**, 150 (1984).
[12] V. Petrov, F. Noack, W. Rudolph, and C. Rempel, Exp. Tech. Phys. (Berlin) **36**, 167 (1988).
[13] F. J. Duarte and J. A. Piper, Opt. Commun. **43**, 303 (1982).
[14] F. J. Duarte, Opt. Quantum Electron. **19**, 223 (1987).
[15] F. J. Duarte, Opt. Quantum Electron. **24**, 49 (1992).
[16] J. Ye and S. Cundiff, *Femtosecond Optical Frequency Comb: Principle, Operation and Applications* (Springer, New York, 2005).
[17] F. W. Helbing, G. Steinmeyer, and U. Keller, Laser Phys. **13**, 644 (2002).
[18] J.-C. Diels, J. Jones, and L. Arissian, in *Femtosecond Optical Frequency Comb: Principle, Operation and Applications*, edited by J. Ye and S. Cundiff (Springer, New York, 2005), Chap. 3, pp. 333–354.
[19] K. W. Holman, D. J. Jones, J. Ye, and E. Ippen, Opt. Lett. **28**, 2405 (2003).
[20] T. H. Yoon, S. T. Park, E. B. Kim, and J. Y. Yeom, IEEE J. Sel. Top. Quantum Electron. **9**, 1025 (2003).
[21] In performing such an analysis, care must be taken to define the optical path as connecting two real optical phase fronts, and not from a phase front to an arbitrary surface.
[22] CVI, 200 Dorado Place, Albuquerque, P.O. Box 11208, ABQ, NM 87192.